Thermochimica Acta, 180 (1991) 269–280
Elsevier Science Publishers B.V., Amsterdam

KINETICS OF OXIDATION OF Cr_3B_4 CERMETS CEMENTED BY DIFFERENT METALLIC BINDERS. Part I. Using iron as a binder

S.S. YOUNIS, A.M. KHATER, M.A. EL MASRY, A.N. MAHDY and M.F. ABADIR
Faculty of Engineering, Cairo University, Giza (Egypt)

(Received 21 August 1990)

ABSTRACT

Experimental work was carried out to study the effect of time, temperature and percentage by weight of binder on the mechanism of oxidation of Cr_3B_4 in air. The material was prepared in the form of pressed cylinders with the binder content varying from 1 to 20 wt.%. The temperature ranged from 400 to 1000 °C (in 100 °C steps) with time intervals of up to 5 h. It was found that the amount of weight gain due to oxidation increases with increasing time and temperature, and decreases with increasing binder content. The oxide film thickness was measured at different temperatures. The mechanism of oxidation and the rate-controlling steps were determined. The activation energy for initial oxidation was also calculated. It was found that increasing the binder content increases thermal stability.

INTRODUCTION

Owing to their physical and high mechanical properties, which remain unchanged at elevated temperatures, borides are widely used in industry as materials for thermocouple jackets, crucibles, cutting tools, jets of aeroplanes and rockets etc. [1]. Because chromium boride is a brittle material, some metal must be added to introduce some ductility. The oxidation stability of these materials should also be taken into consideration when they are used at high temperatures. The extent of application of the chrome borides is still limited by the lack of reliable data on their high temperature behaviour [2]. The aim of this work is to study the effect of different process variables on the kinetics of oxidation of chrome boride cermet materials.

PREVIOUS WORK

The high temperature oxidation of some borides has already been investigated [3–5]. However, these studies were carried out under different

0040-6031/91/$03.50

conditions and therefore it is impossible to compare the results obtained from different experiments.

Cr_4B remains unoxidized below 900 °C owing to the formation of a Cr_2O_3 protective film [6]. Cr_2B, however, is completely oxidized at 800 °C [6], giving Cr_2O_3 and chrome oxyboride. This is almost identical with the oxidation of Cr_3B_2 [6].

Similarly, the oxidation of CrB is hindered at low temperatures (below 800 °C in air) owing to the formation of a protective oxyboride layer which breaks up at about 1000 °C, and after a few hours, re-forms as Cr_2O_3 which enhances the protective action [6]. For Cr_3B_4, it was observed that appreciable decomposition begins at 600–700 °C with the direct formation of a Cr_2O_3 film together with B_2O_3. It was claimed that the latter oxide plays a role in preventing oxidation at higher temperatures.

CrB_2 compacts oxidize at temperatures as low as 600 °C with the formation of B_2O_3 and Cr_2O_3. The rate of oxidation increases sharply at 1150 °C and peeling of the pellets takes place at 1200 °C. At this temperature, oxidation is pronounced and different chromium oxides are formed. Owing to the volatilization of B_2O_3, only traces remain at that temperature [6,7].

Effect of binding materials

The borides of the transition metals are characterized by high oxidation resistance. Adding a metal binder increases the toughness of the boride and hence improves the mechanical strength of the compact. However, the presence of a metal decreases its hardness; therefore a compromise should be made between hardness and toughness [8]. On the other hand, the presence of a metal binder accelerates densification during sintering. In general, the addition of a binding material (Fe–Ni–Co) improves the thermal resistance of transition metal borides.

EXPERIMENTAL

The thermal stability of chrome boride cemented by iron was investigated. The sample was prepared in the form of cylindrical compacts produced by hot pressing of Cr_2O_3 and B_2O_3 powders (Analar grade) in argon at 1400 °C, at a pressure of 2000 lbf in^{-1}, and at pressing times of up to 60 min. The binder content in the compacts varied from 1 to 20 wt.%. The experiments covered a temperature range of 400–1000 °C in 100 °C steps. Scanning electron microscopy was used to investigate the microstructure before and after oxidation. X-ray identification was used to monitor the different phases appearing on heating or cooling different mixtures of oxides. The pressed compacts were found to consist of Cr_3B_4 grains cemented at their grain boundaries with iron crystals.

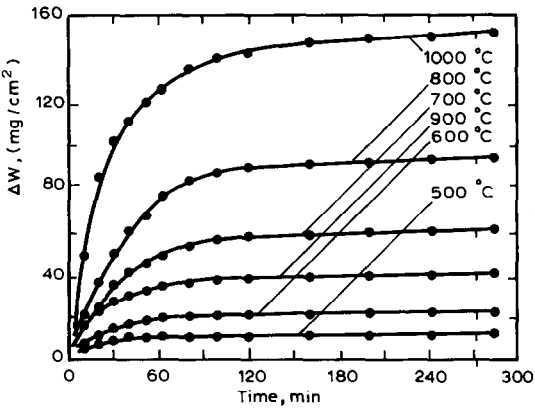

Fig. 1. Kinetic oxidation curves for Cr_3B_4–1 wt.%Fe at different temperatures.

Effect of time and temperature on oxidation of Cr_3B_4–Fe cermets

The effect of time on the weight gain per unit area, Δw (mg cm^{-2}) of 1 wt.%Fe–99 wt.%Cr_3B_4 compacts at different temperatures is shown in Fig. 1. Other curves drawn for higher percentages of iron show a similar pattern. It is clear from the figure that no weight gain occurs below 500 °C. On increasing the temperature of oxidation, the weight gain per unit area increases; at 900 °C, the weight gain per unit area is lower than that at 700 and 800 °C; above 1000 °C, partial melting of the sample takes place. The oxidation curves follow the following general pattern (the oxidation behaviour at 1000 °C is considered as an example). The curves may be divided into three stages:

1. Initial stage: roughly up to 30 min. This stage is characterized by a high constant rate of oxidation.
2. Intermediate stage: roughly between 30 and 110 min. Throughout this stage, the rate of oxidation decreases.
3. Final stage: roughly above 110 min. The rate of oxidation in this stage is the slowest compared with the initial and intermediate stages.

Effect of percentage by weight of binder on oxidation of Cr_3B_4–Fe cermets

The effect of the percentage by weight of binder on Δw was studied at temperatures ranging from 500 to 1000 °C. Figures 2 and 3 show the curves corresponding to the minimum and maximum temperatures respectively. It is clear that the stability towards oxidation increases with increasing the percentage by weight of iron. At 500 °C, pellets containing more than 12 wt.% Fe did not oxidize, while at 1000 °C slight oxidation was observed up to 20% binder content.

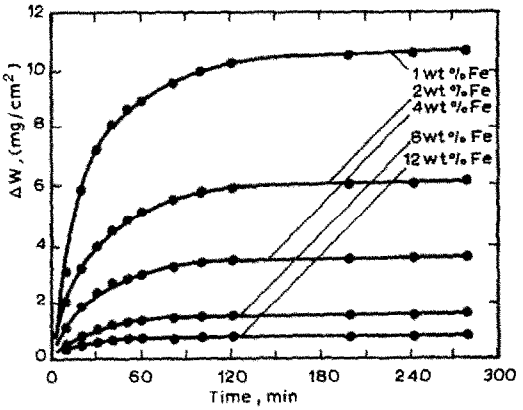

Fig. 2. Isothermal oxidation curves for Cr_3B_4, 1–12 wt.%Fe at 500 °C in air.

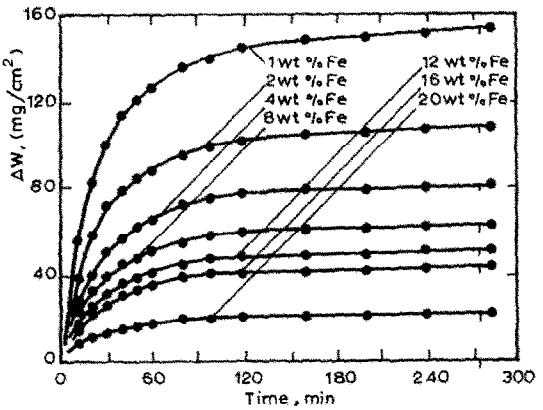

Fig. 3. Isothermal oxidation curves for Cr_3B_4, 1–20 wt.%Fe at 1000 °C in air.

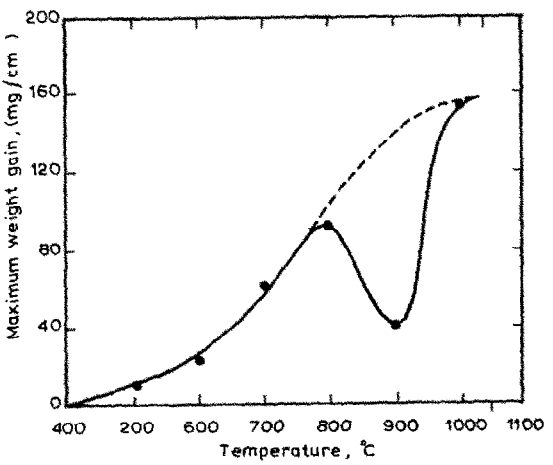

Fig. 4. The effect of temperature on the maximum weight gain of Cr_3B_4–1 wt.%Fe.

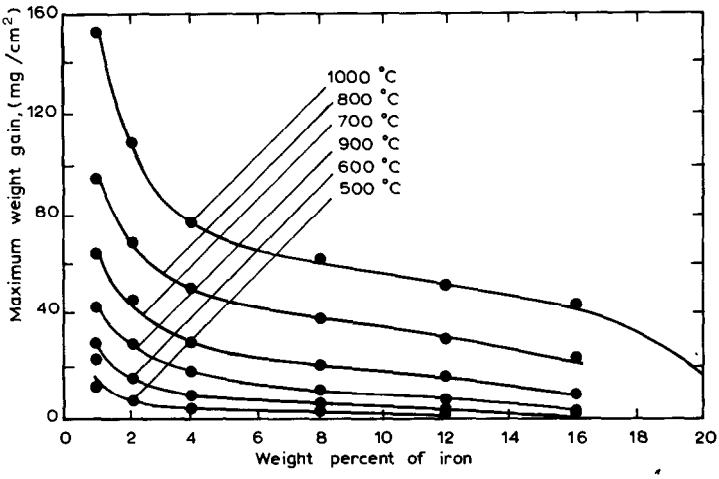

Fig. 5. The effect of iron content on the maximum gain in weight of Cr_3B_4–Fe cermets at different temperatures.

Effect of temperature on the maximum weight gain

The effect in Fig. 4 is typical of all curves: unusual behaviour was observed at 900 ° C where the maximum weight gain is much lower than was expected.

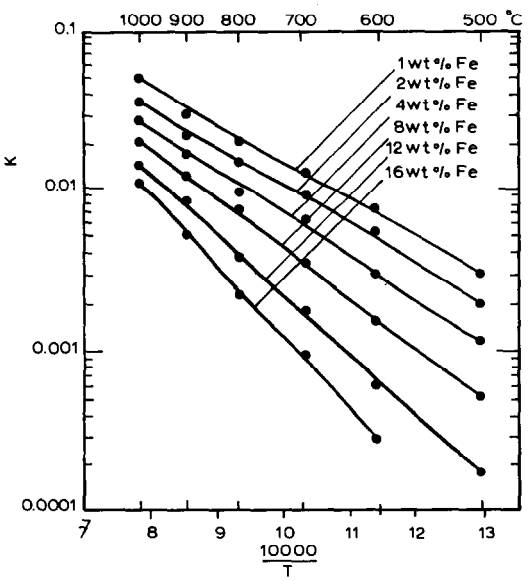

Fig. 6. Rate constant K vs. $(1/T \times 10^4)$ of Cr_3B_4–Fe cermets for different iron contents.

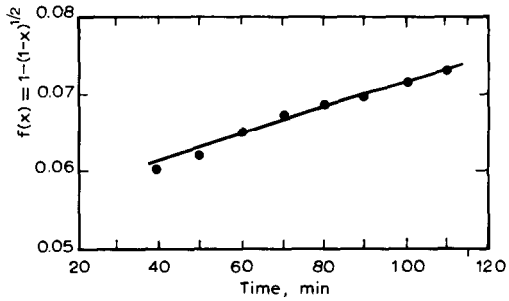

Fig. 7. Intermediate stage of oxidation: $f(x)/t$ relationship assuming phase boundary motion-controlling for Cr_3B_4–1 wt.%Fe at 1000 °C.

Effect of binder content on the maximum weight gain

This effect is shown in Fig. 5, from which it can be observed that the maximum weight gain per unit area decreases with increasing percentage by weight of binder. Also, it is clear from the figure that the maximum weight gain increases with increasing oxidation temperature. All curves tend to reach a high oxidation stability, regardless of the temperature used, at 20 wt.% Fe.

Isothermal kinetics of oxidation of compacts

As has been shown, there are three stages of oxidation. In the initial stage, where the rate of oxidation is constant (Fig. 1), the relation between weight gain per unit area and time in minutes may be represented by

$$\frac{dw}{dt} = K \tag{1}$$

This is a zero-order reaction. The values of the reaction constant K at

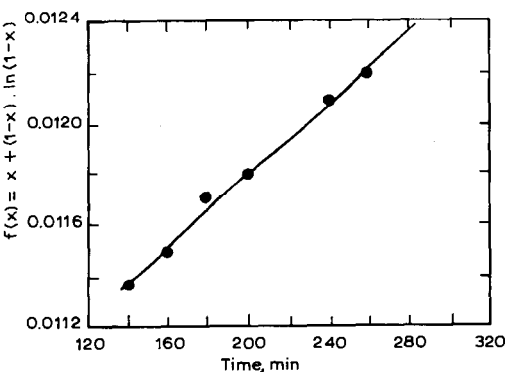

Fig. 8. Final stage of oxidation at 1000 °C: $f(x)/t$ relationship assuming two-dimensional diffusion rate-controlling for Cr_3B_4–1 wt.%Fe.

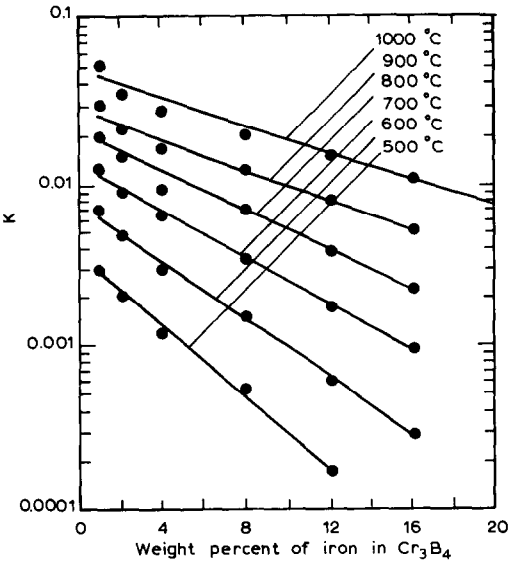

Fig. 9. Rate constant K vs. percentage of iron.

different temperatures and different percentages by weight of iron are shown in Fig. 6.

In the next stage, a straight-line relationship can be obtained by plotting $f(x)$ vs. t (Fig. 7) where

$$f(x) = 1 - (1 - x)^{1/2} = K_1 t \tag{2}$$

This stage of oxidation may be considered a phase-boundary rate-controlling reaction (cylindrical symmetry) [10].

At the final stage of oxidation, as shown in Fig. 8, a straight line relation between $f(x)$ and t is obtained when $f(x)$ satisfies the relation

$$f(x) = (1 - x)\ln(1 - x) + x = K_2 t \tag{3}$$

We conclude that the third stage of oxidation may be considered a two-dimensional diffusion rate-controlling reaction (cylindrical symmetry) [10].

*Effect of binder content on the reaction constant (*K*) (initial stage)*

This effect is shown in Fig. 9. From the curve it is observed that the reaction constant decreases with increasing binder content. A logarithmic relation between K and iron content at 1000 °C was obtained:

$$\ln K = -1.2 - 0.1025\ \alpha \tag{4}$$

where α is the percentage by weight of iron. Substituting for $\alpha = 0$ gives $K = 0.3$ g min^{-1}. This represents the value of K (initial rate of reaction) of Cr_3B_4 for a hypothetical compact without binder.

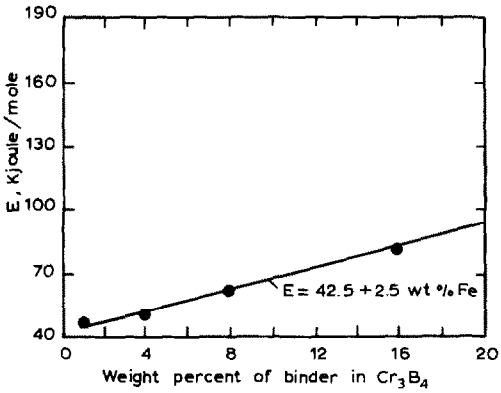

Fig. 10. Activation energy of oxidation for compacts.

Calculation of activation energy during the initial stage of oxidation

It is well known that the rate constant K is defined according to the Arrhenius equation as $K = A\ e^{-E/RT}$. Hence

$$\ln K = \ln A - \frac{E}{RT} \tag{5}$$

A plot of ln K against $1/T$ gives a straight line as has been shown in Fig. 6. The slope of any of these lines is $-E/R$. The activation energy of oxidation of each compact was calculated. The relation between the activation energy E and the percentage by weight of iron is shown in Fig. 10. A correlation was sought between the increase in E and the increase in binder content. We believe that the metal binder offers a resistance towards the motion of the O^{2-} ions which cause the oxidation. This will increase the required activation energy for oxidation in the initial stage of oxidation. If α is the percentage by weight of iron (binder) then, using least-squares analysis, it was possible to obtain the following relation for Cr_3B_4–Fe:

$$E = 42.5 + 2.5\ \alpha \tag{6}$$

where E is in kilojoules per mole. At $\alpha = 0$, $E \approx 42$ kJ mol^{-1}, which represents oxidation of pure Cr_3B_4 compacts.

Metallography and scanning electron microscopy (SEM)

A metallographic section of a polished Cr_3B_4–1 wt.%Fe sample before oxidation shows that two phases are present: a light grey phase and a dark phase. The SEM photograph of the same sample before oxidation also shows the two phases with black areas which represent porosity. The SEM photograph of Cr_3B_4–1 wt.%Fe after oxidation at 900 °C for 5 h shows that the oxide film is continuous with no cracks and has a rough surface. Samples were also examined following oxidation at 800 °C for 5 h: the thickness of

the oxide film at 800 °C was found to be greater than that at 900 °C, while it was thickest at 1000 °C. This indicates that the extent of oxidation at 900 °C is lower than at 800 or 1000 °C, as was also shown in the weight gain–time curves.

Effect of binder content on the thickness of oxide film

Oxidized samples of Cr_3B_4–1 wt.%Fe, up to 20 wt.% Fe, were polished and investigated under the metallograph. It was found that two oxide layers were formed, except for 20 wt.% Fe at 800 °C, where only one layer was found. It was also observed that the thickness of the two oxide layers decreases with increasing binder content. The outer layer was green and the inner was dark grey.

X-ray diffraction analysis

The X-ray diffraction patterns for Cr_3B_4–1 wt.%Fe oxidized at 800, 900 and 1000 °C showed no strong peaks, indicating that the oxide layer has poor crystallinity. At 900 °C, sharp peaks of Cr_2O_3 were found. The metallography of this sample indicated that the oxide film was thin and crystalline which supports the X-ray diffraction results.

In view of the previous results, we believe that the oxidation of Cr_3B_4 compacts proceeds through the formation of Cr_2O_3 and chrome oxyboride at temperatures between 700 and 800 °C. The crystals are not well developed, as demonstrated by the poor crystallinity observed at 800 °C in the X-ray diffraction analysis, but two layers can be distinguished. At 900 °C, the oxyboride layer decomposes, while the Cr_2O_3 crystals grow coarser; B_2O_3 is evolved as a vapour, which explains the sudden decrease in weight gain observed at 900 °C, the well-defined X-ray pattern of Cr_2O_3 and the thickness of the lower layer. Decomposition of the oxyboride leaves a porous Cr_2O_3 layer. Above 900 °C, there are two layers of Cr_2O_3 with different porosities. The outer layer is poorly crystalline because of the newly formed crystals: this accounts for the diffuse X-ray pattern observed at 1000 °C.

Relation between the thickness of the inner layer (Cr_2O_3) and iron content

According to the previous findings, an attempt was made to correlate the thickness of the Cr_2O_3 inner layer (as measured from metallographic sections) with the percentage by weight of iron. The kinetic equation during oxidation of Cr_3B_4 at 800 °C and time t (hours) is

$$\left[1-(1-x)^{1/2}\right] = Kt = At\ e^{-E/RT} \tag{7}$$

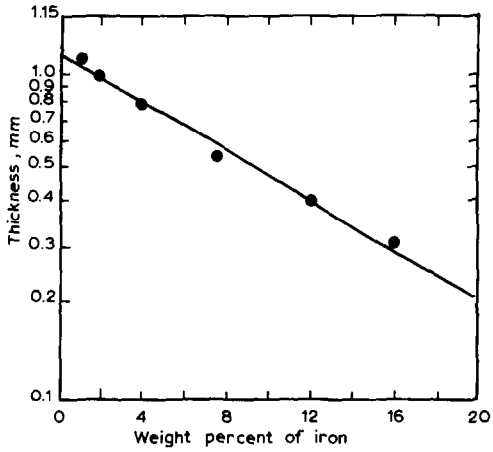

Fig. 11. The relationship between the inner layer thickness and the percentage by weight of binder at 800 °C.

and

$$x = 1 - \left(\frac{r}{r_0}\right)^2 \tag{8}$$

Hence

$$1 - \frac{r}{r_0} = \frac{r_0 - r}{r_0} = \frac{d}{r_0} = At\ \mathrm{e}^{-E/RT} \tag{9}$$

At constant time and constant temperature

$$d = d_0\ \mathrm{e}^{-E/RT} \tag{10}$$

where r_0 is the initial radius and $r = r(t)$
Hence

$$\ln\ d = \ln\ d_0 - \frac{E}{RT} \tag{11}$$

As previously assumed in the initial oxidation stage, we may set E to be $(42.5 + 2.5\ \alpha)$. Therefore

$$\ln\ d = \ln\ d_0 - \frac{42.5}{RT} - \frac{2.5\ \alpha}{RT} \tag{12}$$

and

$$\ln\ d = C - \frac{2.5\ \alpha}{RT} \tag{13}$$

If $\ln\ d$ is plotted against α, a straight line should be obtained. This plot is shown in Fig. 11; the straight line supports the previous model.

CONCLUSION

The oxidation of chrome boride cermets cemented with iron showed that the extent of oxidation increases with temperature, except at around 900 °C, and decreases with the iron content (wt.%). This has been explained using different methods. The kinetic parameters have been related to the iron content. The activation energy of the early stage of oxidation has been found to increase with increasing iron content.

REFERENCES

1 L.J. Bonis and H.H. Hausner, Perspectives in Powder Metallurgy, Fundamentals, Methods and Application, Vol. 1, Plenum, NY, 1967.
2 Yu. Borisov, J.N. Gorbatov, V.R. Kalinovskii, V.K. Fedsrenko, Z.P. Shurygina, N. Kokorina and V. Gopienko, Poroshk. Metall., 22(10) (1985) 50.
3 R.B. Kotelnikov, in Technology of Non-ferrous Metals (in Russian), Nauchn. Tr. Minstsretnetzolota, No. 29, Metallurgizdat, Moscow, 1958, p. 339.
4 G.A. Meerson, G.V. Samsonov and K.I. Portnoi, in Boron, Transactions of a Conference on the Chemistry of Boron and its Compounds (in Russian), Goskhinizdat, Moscow, 1958, p. 58.
5 R. Steinitz, I. Binder and D. Maskovits, J. Met., 4 (1952) 983.
6 M.D. Lyutaya and T.I. Serbryakova, Institute of Materials Science Problems, Academy of Sciences, Ukrssr, Neorganickeskie Materialy, 1(7) (1965) 1044.
7 R.F. Voitovich, A Handbook of the Thermodynamic Characteristics of Refractory Compounds, Naukova Dumka, Kiev, 1971.
8 A.G. Evans, in S.W. Freeman (Ed.), Fracture Mechanics Applied to Brittle Materials, American Society for Testing and Materials, ASTM STP 678, 1979, pp. 112–135.
9 M.S. Koval Chenko and L.F. Ochkas, The Kinetics of Densification of Binary Titanium–Chromium Diboride with Copper–Nickel Binder, Institute for Problems of Materials Science, Academy of Sciences of the Ukrainian SSR, Kiev, USSR, (1981).
10 W.W. Wendlandt, Thermal Methods of Analysis, Wiley, New York, 2nd edn., 1974.

APPENDIX: NOMENCLATURE

A	pre-exponential factor
C	dimensionless constant
d	thickness of oxide layer (mm)
d_0	initial thickness of oxide layer (mm)
E	activation energy (kJ mol^{-1})
K	rate constant (early stage of oxidation) (g min^{-1})
r	radius of cylindrical pellet (mm)
r_0	initial radius of cylindrical pellet (mm)
R	general gas constant (J mol^{-1} K^{-1})
t	time (min)

T temperature (K)
x conversion

Greek symbols

α percentage by weight of iron
Δw gain in weight per unit area (mg cm^{-2})